

CAWM IV AND V MODELS – DESCRIPTIVE MEMORANDUM

José Almir Cirilo

Head Professor at UFPE, Agreste Campus

almir.cirilo@gmail.com

The development of CAWM – Agreste Campus Watershed Model initially aimed to simulate surface runoff in watersheds of semi-arid regions, aiming to fill the gap regarding this type of model, taking advantage of the potential of more modern data input and output procedures and the possibility of utilizing information generated by geoprocessing techniques on spatial databases such as SRTM – Shuttle Radar Topography Mission and the Pernambuco Tridimensional Program, PE3D.

One of the premises sought in the development of CAWM is simplicity and few parameters to calibrate, whenever possible with physical significance.

1. THEORETICAL FOUNDATIONS OF CAWM IV

The physical processes represented in the CAWM IV model are indicated in Figure 1.

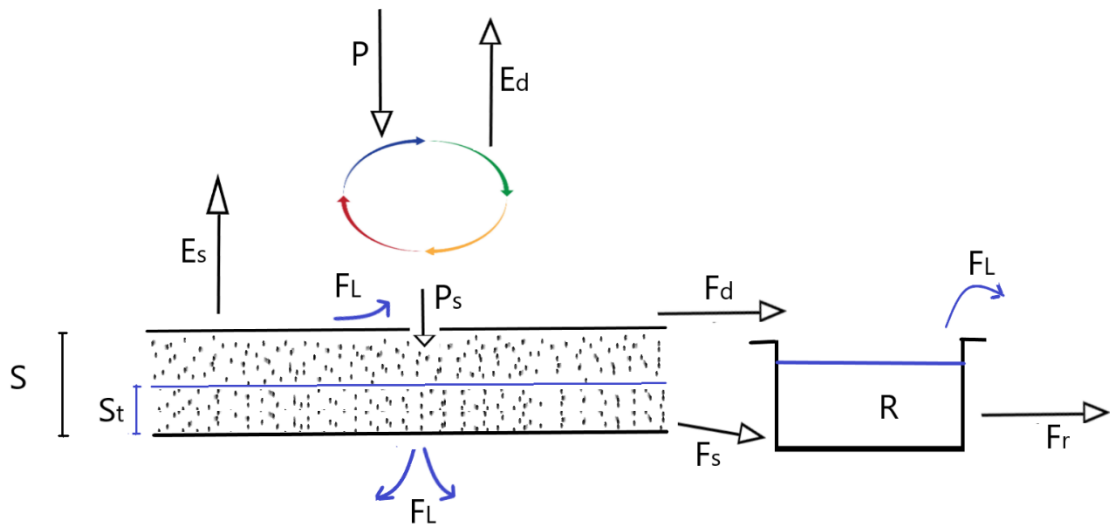


Figure 1 - Schematic representation of the CAWM IV model.

In this model, the precipitation-evapotranspiration potential balance is initially made by comparing their values. If there is sufficient precipitation, the potential evapotranspiration (E) is immediately deducted. The excess is the effective precipitation (P_n). Otherwise, all precipitation is consumed as direct evapotranspiration (E_d), and the unmet portion (E_n) can be fully or partially extracted from the soil reservoir if there is sufficient water for it. The balance is described by the following expressions:

$$\text{If } P \geq E, \text{ then } P_n = P - E \quad (1)$$

$$\text{If } P \leq E, \text{ then } E_d = P \text{ e } E_n = E - E_d \quad (2)$$

The effective precipitation is divided into three components. The first one refers to soil recharge (P_s), based on the concept presented by Edijatno and Michel (1989), according to Equation 3:



$$P_s = \frac{s \cdot \left(1 - \left(\frac{S_t}{S}\right)^2\right) \cdot \tanh\left(\frac{P_n}{S}\right)}{1 + \frac{S_t}{S} \tanh\left(\frac{P_n}{S}\right)} \quad (3)$$

Where S_t is the amount of water accumulated in the soil at each time step and S is its maximum retention capacity. The concept of P_s is used in the formulation of the GR4J lumped model (PERRIN *et al.*, 2003; NASONOVA, 2011; TRAORE *et al.*, 2014).

Another component is supplemental evapotranspiration (E_s), limited to the unmet evapotranspiration E_n , provided that there is sufficient water. Its magnitude depends on a value assigned to a parameter α as indicated in Equation 4. This parameter was introduced due to uncertainties in evapotranspiration estimation, including the fact that soil conditions, vegetation cover, and climate vary within the watershed area.

$$E_s = \left(1 - e^{-\frac{\alpha \cdot S_t}{S}}\right) \cdot E_n \quad (4)$$

The remaining component, if positive, represents direct surface runoff (F_d) according to Equation 5:

$$F_d = P_n - P_s - E_s \quad (5)$$

From the soil water reservoir, the subsurface flow F_s occurs, which percolates until increasing the water volume in the river channel (R), according to Equation 6:

$$F_s = K_s \cdot S_t \quad (6)$$

Where K_s is a calibrated parameter representing the soil permeability. F_s indicates percolation towards the river channel.

The water volume retained in the river channel is increased by the flows F_s and F_d . The flow in the river channel F_r is assumed to be a nonlinear function of the stored volume R , according to Equation 7, where b is a constant to be determined and K is a parameter depending on watershed characteristics.

$$F_r = K \cdot R^b \quad (7)$$

Considering that the volume of the river channel reservoir V_{sup} can be represented by the capacity of the rivers that make up the watershed with a total length L_T and an equivalent cross-sectional area A_e , there is:

$$V_{sup} = A_e \cdot L_T \quad (8)$$

Since in hydrological models, volumes are represented in millimeters per unit area of the watershed in km^2 , the accumulation R is given by:

$$R = \frac{V_{sup}}{c \cdot A_b} = \frac{A_e \cdot L_T}{c \cdot A_b} \quad (9)$$



Being the constant $c = 1000$ used to reconcile the units used.

Considering the flow in the channel described by the Manning Formula with simplifications of a rectangular section with equivalent width B_e , a section of extension L_T and a slope S_0 , as well as a hydraulic radius approximately equal to the flow depth:

$$A_e = B_e \cdot y \quad R_h \cong y$$
$$Q = \frac{1}{n} \cdot A_e \cdot R_h^{2/3} \cdot S_0^{1/2} \cong \frac{1}{n} \cdot \frac{A_e^{5/3}}{B_e^{2/3}} S_0^{1/2} \quad (10)$$

Considering $V = A_e \cdot L_T$ s the volume of water accumulated in the fluvial channel in a section of extension L_T and equivalent area A_e , there is, substituting into Equation 10:

$$Q = \frac{S_0^{1/2}}{n \cdot L_T^{5/3} \cdot B_e^{2/3}} V^{5/3} = K^* \cdot V^{5/3} \quad (11)$$

By similarity, Equation 11 suggests $b = 5/3$ when compared to Equation 7. The relationship between flow rate (m^3/s) and flow depth (mm) is given by:

$$Q = \frac{F_r \cdot c \cdot A_b}{\Delta t} \quad (12)$$

where Δt is the time step in seconds. Combining Equation 12 with the last term of Equation 10, there is:

$$\frac{F_r \cdot c \cdot A_b}{\Delta t} = \frac{1}{n} \cdot \frac{A_e^{5/3}}{B_e^{2/3}} S_0^{1/2} \quad (13)$$

Explicitly expressing the equivalent area from Equation 9 and substituting into Equation 13, there is:

$$A_e = \frac{c \cdot A_b \cdot R}{L_T} \quad (14)$$

$$\frac{F_r \cdot c \cdot A_b}{\Delta t} = \frac{1}{n} \cdot \left(\frac{c \cdot A_b \cdot R}{L_T} \right)^{5/3} \frac{S_0^{1/2}}{B_e^{2/3}} \quad (15)$$

Where $F_r = K \cdot R^b$ and Considering $b = 5/3$, there is:

$$K = \frac{\Delta t}{n} \cdot \left(\frac{c^2 \cdot A_b^2}{B_e^2 \cdot L_T^5} \right)^{1/3} S_0^{1/2} \quad (16)$$

The K parameter can also be calculated simply through the watershed area. The nonlinear relation $F_r = K \cdot R^b$ indicated in Equação 7 is used in CAWM to represent flow in the fluvial channel, different from the usual concept of a linear reservoir. The deduced expression indicates the possibility of calculating the parameter K and considering $b = 5/3$, although there are many simplifications made in the mathematical development. The value $b = 5/3$ has been well-adjusted in simulations for dozens of watersheds. The calculation results of the

parameter K have been evaluated for different basins, with simulations in daily time steps, as discussed below.

Water losses in the system can be due to various causes: retention volumes in soil depressions and vegetation, gradually evaporated; overflow volumes that do not return to the fluvial channel, also evaporated; infiltration into cracks in the crystalline basement. This loss is subtracted from the direct surface runoff. The following expression is used to calculate losses:

$$F_L = K_L \cdot R^p \quad (17)$$

The exponent p has been tested in various simulations, ranging from 1 to 2. In most cases, the value 1 is more appropriate, being the default value of the model. Only in areas with large overflows, a higher value is more suitable. The parameter of losses, K_L , can be calculated from the first simulation, considering the values of the generated global balance:

$$K_L = \frac{V_{Prec} - V_{Qobs} - V_{Evap}}{V_{Prec} - V_{Evap}} \quad (18)$$

The parameter to calibrate in the CAWM IV model is therefore K_S . The parameter K is suitable in the range of 0.01 to 0.06, with a reference value of 0.025. In the case of rivers with steep slopes, the calculated value from Equation 16 is generally higher. If this occurs, it is recommended to exclude the steepest sections of the river course when calculating the slope. On the other hand, in very large basins, the total length of the river network LT can result in K values well below the range that yields better results. In situations where the parameter value falls outside the recommended range, $K = 0.025$ has been used.

The parameter S is estimated as the water retention capacity in the soil, calculated from the average Curve Number (CN) of the basin:

$$S = 254 \left(\frac{100}{CN} - 1 \right) \quad (19)$$

Soil mappings from EMBRAPA and classified satellite images of land use and land cover in the basins have been used for CN calculation. A plugin has been developed and incorporated into the QGIS software for this purpose. Figures 2 and 3 below illustrate soil mapping, land use, and land cover in selected basins in Pernambuco for CN calculation.

In the absence of the necessary information, K and S can be calibrated. However, this approach has been avoided to incorporate more measurable information about the characteristics of the study areas into the model.

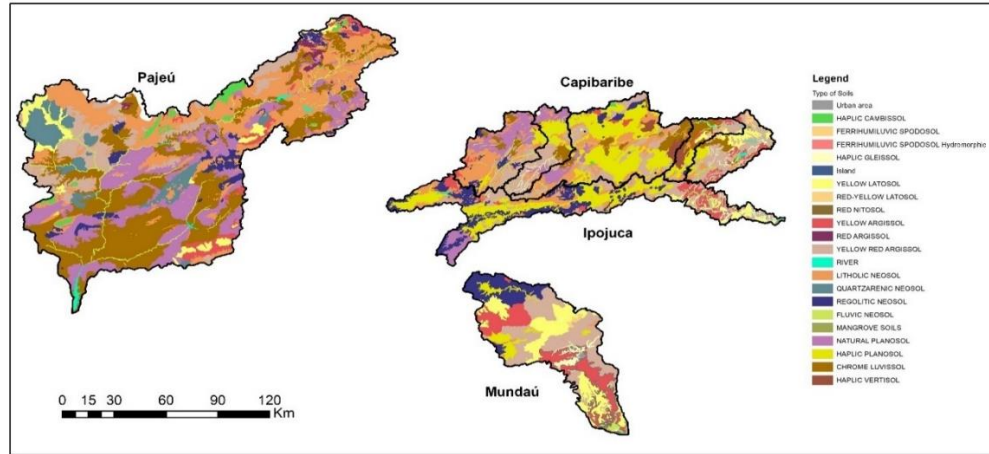


Figure 2 - Soil mapping for three watersheds in Pernambuco. Source: Cirilo *et al.*, 2020.

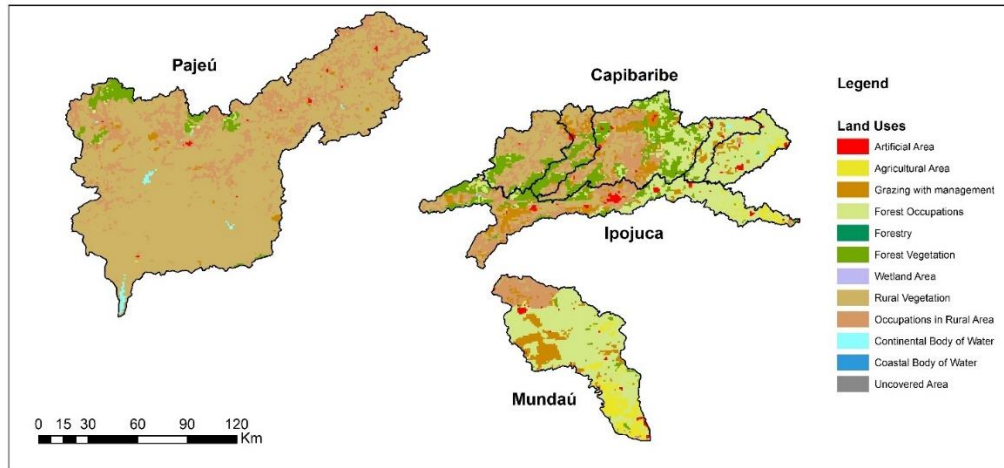


Figure 3 - Classified images of land use and land cover for three watersheds in Pernambuco. Source: Cirilo *et al.*, 2020.

2. VERSION CAWM V

The CAWM V model aims to incorporate the flow processes in perennial river basins, in regions with deeper soils that allow the maintenance of base flows during dry periods. The main change compared to CAWM IV is the addition of an underground reservoir that is replenished when the soil reservoir reaches saturation (Figure 4). From that point on, a flow of deep percolation P_g begins to replenish the groundwater reservoir, adding to the accumulated water depth G . The flow F_g is then extracted from the groundwater reservoir and contributes to the river flow, complementing the components F_d and F_s :

$$F_g = K_g \cdot G \quad (20)$$

Where K_g is a parameter representing water transfer in the soil, similar to K_s . To allow the replenishment of the underground reservoir, the calculation formula for percolation P_s has been modified to:

$$P_s = P_n \cdot \left(1 - \frac{S_t}{\beta \cdot S}\right) \quad (21)$$

Pernambuco, the Three-Dimensional Pernambuco Program (PE3D) is available, which had its beginnings shortly after the catastrophic flood that destroyed cities in Pernambuco and Alagoas in 2010. During the operation of the crisis committee established by the state government, a team from the National Water Agency (ANA) presented to the proposer, who was then responsible for water resources management in Pernambuco, the possibility of using laser scanning technology for terrain identification as a fast and accurate way to conduct the necessary topographic surveys for the implementation of flood containment works, reconstruction, and city planning.

The work was carried out and quickly supported the development of dam projects, river channel expansion and reordering, land eviction, and riverbank revitalization in urban areas, studies and research on risks, and necessary actions to minimize the effects of flooding. These actions, combined with an efficient monitoring network and the operation of the Serro Azul Dam, the largest among the projects initiated in the Una River basin (the basin most affected by historical floods in the Mata Sul region of Pernambuco), significantly reduced the impact of the flood that occurred in the region in May 2017, when the accumulated precipitation exceeded, in less time, the rainfall from the 2010 event.

After the prototype of laser surveying for 1,100 km² along three rivers where the flooding was most severe in 2010, there was an initiative to expand the survey to cover the entire 98,500 km² territory of the state. This work, completed in December 2016, gave rise to the Three-Dimensional Pernambuco Program, the only high-resolution laser-based territorial database generated in a Latin American state. The contracted services included aerial photogrammetric coverage and laser profiling of the entire state of Pernambuco. The state was divided into 13,125 articulated sheets. For each of the articulations, a set of products was developed through aerial photogrammetric coverage at a scale of 1:5,000 and another using LiDAR technology. From the aerial photogrammetric coverage, orthophotos were generated at a scale of 1:5,000 with a spatial resolution of 50 cm, as well as photo indices and their respective metadata. For laser profiling, the products consist of Hypsometric Intensity Images, Digital Elevation Models (DEM), and Digital Terrain Models (DTM) in a text file format with the "x, y, z" coordinates of each point, as well as in GeoTIFF format, which is the usual standard for this type of product. The density of surveyed points is approximately 3 points per 4 m². The generated database contains elevation values for approximately 75 billion points in the territory of Pernambuco.

Additionally, the urban areas of the headquarters of 41 municipalities were mapped at a scale of 1:1,000. These urban areas have a total approximate area of 870 km², and the spatial resolution of the orthophotos is around 12 cm. For the laser profiling of these cities, the acceptable altimetry error was less than 10 cm, while the average density of the survey is approximately 4 points/m².

Due to the quality of the database and the extent of the survey, PE3D has been used in the development of studies, projects, and numerous research works. Hydrodynamic modeling, in particular, has benefited from the improved terrain resolution (RIBEIRO *et al.*, 2020; OLIVEIRA *et al.*, 2019; RIBEIRO NETO *et al.*, 2015; DANTAS *et al.*, 2014). For the hydrological simulation in larger areas, the computational effort in generating the physical elements is very high, leading to the resampling of surveyed points to larger spacing intervals (e.g., 5m).

In the case of simulations for watersheds in other states, obtaining physical parameters for CAWM is done using data from the Shuttle Radar Topography Mission (SRTM) database (accessible at <https://www.usgs.gov/centers/eros>) and classified images available for the study areas.

5. SENSITIVITY OF PARAMETERS

The exponent "p" has been tested in various simulations, ranging from 0.7 to 1.2. In most cases, the value of 1 has proven to be more suitable and serves as the default value for the model. Only areas with significant overflows have a higher value shown to be more appropriate.

The parameter "K" has shown to be suitable for a variation between 0.01 and 0.07, with a reference value of 0.025. In the case of rivers with steep slopes, the calculated value from Equation 17 is usually higher. If this happens, it is recommended to exclude the steeper sections of the river course when calculating the slope. On the other hand, in very large basins, the total length of the river network, L_T , may result in K values below the range that yields better results.

An analysis of 109 basins led to the following expression for calculating K based on the area:

$$\begin{cases} \text{If } Area \leq 1,500 \text{ km}^2, K = 0.3745 \cdot A^{-0.489} + 0.0146 \\ \text{If } 1,500 \text{ km}^2 < Area < 60,000 \text{ km}^2, K = 34.343 \cdot A^{-0.853} \\ \text{Otherwise, } K = 0.0028 \end{cases} \quad (22)$$

The value of L_T is also influenced by the resolution of the used Digital Terrain Model (DTM) or Digital Elevation Model (DEM). When using the SRTM database, it is recommended to adopt a threshold between 300 and 500 to define the number of cells in the formation of the drainage network. When using PE3D, which has a much higher resolution, this threshold should be increased to around 5000 to avoid the generation of pseudo watercourses with insignificant extensions.

These recommendations are part of the CAWM model usage tutorial and derive from the experience of the GEOLAB team - Geoprocessing Laboratory of UFPE's Agreste Campus.

The research is being developed with the application of CAWM IV model to the semi-arid watersheds of Northeast Brazil, continuing the work carried out in the parameter regionalization for Pernambuco (CIRILO *et al.*, 2020) with promising results. It also references the analysis conducted by Virões and Cirilo (2019) regarding the parameter regionalization of another model for part of the semi-arid region in Northeast Brazil. On the other hand, the CAWM V model has been applied to watersheds in sub-humid and humid climates in the coastal region of Northeast Brazil, including the basins of major rivers in Maranhão and Piauí. The model is also being applied to watersheds that are part of the São Francisco River, such as successful simulations conducted for the Rio das Velhas basin, indicated in the hydrograph in Figure 5 (precipitation on the right axis).

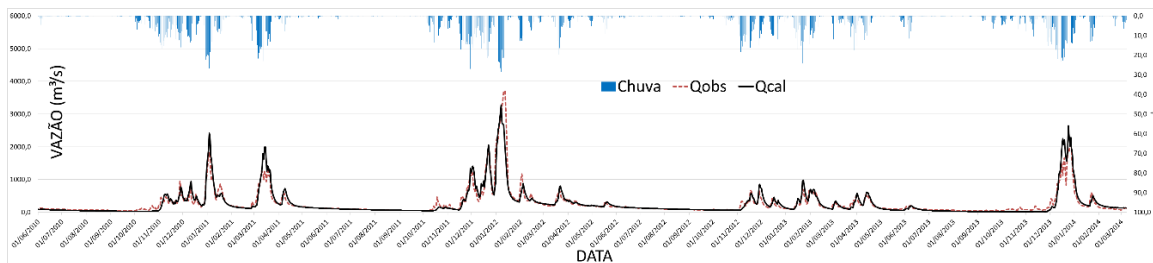


Figure 5 - Daily streamflows recorded and simulated with the CAWM V model for the Velhas River, MG.

6. PERFORMANCE INDICATORS AND PROCEDURES FOR PARAMETER CALIBRATION IN THE MODELS

The performance indicators used in the CAWM IV and CAWM V models are:

- NSE: Nash-Sutcliffe efficiency coefficient and its derivatives NSElogQ and NSEsqrQ;
- R²: coefficient of determination;
- RMSE: root mean square error;
- Pbias%: mean percentage error;
- RSR: ratio of RMSE to standard deviation, Where:

$$NSE = 1 - \frac{\sum_{i=1}^n (Q_{i,obs} - Q_{i,cal})^2}{\sum_{i=1}^n (Q_{i,obs} - \overline{Q_{obs}})^2} \quad (23)$$

$$NSE_{sqrQ} = 1 - \frac{\sum_{i=1}^n (\sqrt{Q_{i,obs}} - \sqrt{Q_{i,cal}})^2}{\sum_{i=1}^n (\sqrt{Q_{i,obs}} - \sqrt{\overline{Q_{obs}}})^2} \quad (24)$$

$$NSE_{logQ} = 1 - \frac{\sum_{i=1}^n (\log Q_{i,obs} - \log Q_{i,cal})^2}{\sum_{i=1}^n (\log Q_{i,obs} - \log \overline{Q_{obs}})^2} \quad (25)$$

$$RMSE = \frac{1}{n} \left[\sum_{i=1}^n (Q_{i,obs} - Q_{i,cal})^2 \right]^{1/2} \quad (26)$$

$$Pbias = \left[\frac{\sum_{i=1}^n (Q_{cal}(i) - Q_{obs}(i))}{\sum_{i=1}^n (Q_{obs}(i))} 100 \right] \quad (27)$$

$$RSR = \frac{\left[\sum_{i=1}^n (Q_{i,obs} - Q_{i,cal})^2 \right]^{1/2}}{\left[\sum_{i=1}^n (Q_{i,obs} - \overline{Q_{obs}})^2 \right]^{1/2}} \quad (28)$$

Where n is the number of data points in the event, $Q_{i,obs}$ is the observed flow, $Q_{i,cal}$ is the calculated flow and $\overline{Q_{obs}}$ is the mean observed flow over the period.

Gotschalk and Motovilov (2000, cited in Van Liew *et al.*, 2007) classified values of NSE above 0.75 as very good, and values between 0.75 and 0.36 as satisfactory, for both daily and monthly flows. Other authors consider values equal to or above 0.5 as acceptable. These references can also be considered for NSE derivatives.

Moriasi *et al.* (2007) recommended the value ranges for NSE, Pbias, and RSR indicated in Table 1.

Table 1. Recommended performance indicators for monthly simulations.

	NSE	Pbias (%)	RSR
Very good	0.75-1.00	< ±10	0-0.5
Good	0.65-0.75	±10 - ±15	0.5-0.6
Satisfactory	0.50-0.65	±15 - ±25	0.6-0.7
No satisfactory	<0.5	>±25	>0.7

Fonte: Moriasi *et al.* (2007).

Several authors, such as Pushpalatha *et al.* (2012) and Traore *et al.* (2014), use these and other variations of NSE as performance indicators. According to Traore *et al.* (2014), higher NSE values indicate better fits for higher flows, NSE_{sqrQ} represents intermediate flows

more appropriately and NSE_{logQ} represents lower flows. Pushpalatha *et al.* (2012) concluded that the most suitable indicator for the entire series is NSE_{sqrtQ} . agreeing with this statement, Patil *et al.* (2014) proposed this indicator as the objective function to be maximized in the parameter calibration process of rainfall-runoff models.

After several tests, the most suitable objective function for CAWM IV and CAWM V models was considered to maximize NSE and simultaneously minimizes the sum of absolute errors between observed and calculated flows, as indicated in Equation 29:

$$F = \frac{NSE \cdot 10^6}{\sum abs(Q_{obs} - Q_{calc})} \quad (29)$$

The model has been used in two versions, one developed in MS Excel spreadsheets and another programmed in the Python language. In the first version, calibration is performed using the Non-Linear Programming Solver GRG algorithm. In the second version, routines from "scipy.optimize.minimize" are used. This latter process is being improved to reduce processing time, possibly using the Particle Swarm Optimization (PSO) method, which has shown greater efficiency in other applications.

7. PARAMETER TRANSFER METHOD

The parameter transfer procedure involves the use of data from the calibrated basin, incorporating some information: the basin area (km²), the total observed flow (mm), and the temporal extension of the historical series (days). The following proportionality analysis is performed to estimate the total observed flow (in millimeters) for the uncalibrated basin necessary for the assessment of losses:

$$Q_{obs,2} = Q_{obs,1} \times \frac{A_2}{A_1} \times \frac{Q_{esp,2}}{Q_{esp,1}} \times \frac{N_2}{N_1} \quad (30)$$

Where:

$Q_{obs,2}$: Estimate of the total observed discharge of the uncalibrated basin (mm)

$Q_{obs,1}$: Total observed flow of the calibrated basin (mm)

A_2 : Uncalibrated basin area (km²)

A_1 : Calibrated basin area (km²)

$Q_{sp,2}$: Specific flow of the uncalibrated basin (L/s/km²)

$Q_{sp,1}$: Specific flow of the calibrated basin (L/s/km²)

N_1 : Size of the calibrated basin historical series

N_2 : Size of the uncalibrated basin time series

For example, the isolines represented in Figure 6 were drawn for the Parnaíba river basin. The estimate of the total observed flow from Equation 33 allows the calculation of the loss coefficient (K_L) through Equation 18.

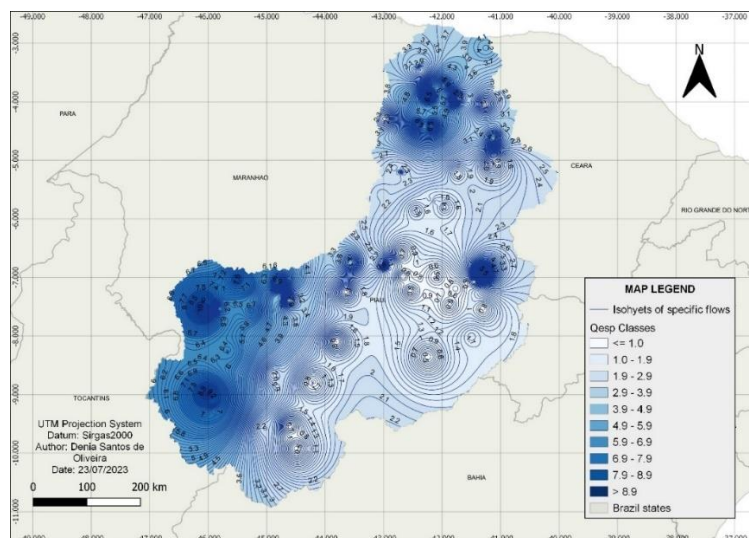


Figure 6 - Map of the isolines with the specific flows of the Parnaíba river basin

The values of the parameters considered as decision variables (K_s and β) obtained from the calibration of the basins are maintained for the analyzed sub-basin.

REFERENCES

- ADAM, E. O.; ELBASIT, M. A. M. A.; TESFAMICHAEL, S.; AHMED, F. Integration of Satellite Rainfall Data and Curve Number Method for Runoff Estimation Under Semi-Arid Wadi System. ISPRS - International Archives of the Photogrammetry, Remote Sensing and Spatial Information Sciences. v. XLII-3/W2, p. 1-7, 2017.
- AL-QURASHI, A.; MCINTYRE, N.; WHEATER, H.S.; UNKRICH, C. Application of the Kineros2 rainfall-runoff model to an arid catchment in Oman. Journal of Hydrology, v. 355, p. 91-105, 2008.
- BÁRDOSSY, A.: Calibration of hydrological model parameters for ungauged catchments, Hydrology and Earth System Science, 11, 703-710, <https://doi.org/10.5194/hess-11-703-2007>, 2007.
- BECK, H. E.; VAN DIJK, A. I. J. M.; DE ROO, A.; MIRALLES, D. G.; MCVICAR, T. R.; SCHELLEKENS, J.; BRUIJNZEEL, L. A.. Global-scale regionalization of hydrologic model parameters. AGU Publications, Water Resources Research, 2016. <https://doi.org/10.1002/2015WR018247>
- BERGSTROM, S. The HBV model - its structure and applications, SMHI Rep. RH 4, Swedish Meteorological and Hydrological Institute, Norrköping, Swed, 1992
- CABRAL, S. L.; SAKURAGI, J.; SILVEIRA, C. S.; Incertezas e erros na estimativa de vazões usando modelagem hidrológica e precipitação por RADAR. Revista Ambiente & Água, v.12, n.1, 2017. Disponível em:<<http://www.scielo.br/pdf/ambiagua/v12n1/1980-993X-ambiagua-12-01-00057.pdf>>. Acesso em: 06 de dezembro de 2017.

- CIRILO, J. A.; VERÇOSA, L. F. M.; GOMES, M. M. A.; FERRAZ, G. F.; SILVA, B. M. (2020) Development and application of a rainfall-runoff model for semi-arid regions. *Brazilian Journal of Water Resources*. v.25, e.15, 1 - 19. DOI: <https://doi.org/10.1590/2318-0331.252020190106>.
- COSTA, V.; FERNANDES, W.; NAGHETTINI, M. Regional models of flow-duration curves of perennial and intermittent streams and their use for calibrating the parameters of a rainfall-runoff model, *Hydrological Sciences Journal*, 59:2, 262-277, 2014. DOI: 10.1080/02626667.2013.802093
- DANTAS, C.E.O.; CIRILO, J. A.; RIBEIRO NETO, A.; SILVA, E. R. Caracterização da Formação de Cheias na Bacia do Rio Una em Pernambuco: Análise Estatística Regional. *Revista Brasileira de Recursos Hídricos*, v.19, p.239 - 248, 2014.
- EDIJATNO; MICHEL, C.. Un modèle pluie-débit journalier à trois paramètres. *La Houille Blanche*, n. 2, p.113-122, 1989.
- FEITOZA, M. A. B. Aplicação de Modelo de Simulação Hidrológica com Regionalização de Parâmetros para Regiões Semiáridas. Dissertação de Mestrado. Pós-Graduação em Engenharia Civil e Ambiental, UFPE, Campus Agreste, Caruaru, PE. 145p, 2021.
- FELIX, V. S.; PAZ, A. R. Representação dos Processos Hidrológicos em Bacia Hidrográfica do Semiárido Paraibano com Modelagem hidrológica Distribuída. *Revista Brasileira de Recursos Hídricos – RBRH*, v.21, n.3, p. 556-569, Porto Alegre, 2016.
- GARAMBOIS, P.A.; ROUXBC, H.; LARNIERBC, K.; LABATD, D.; DARTUSBC, D. Parameter regionalization for a process-oriented distributed model dedicated to flash floods. *Journal of Hydrology*, Volume 525, Pages 383-399, 2015.
- GIRARDI, R. V.; CASTRO, N.; GOLDENFUN, J. A.; SILVEIRA, A. L. L. Avaliação do Efeito de Escala em características de Chuva e Vazão em Sub-Bacias Embutidas da Bacia do Potiribu-RS. *Revista Brasileira de Recursos Hídricos – RBRH*, v.16, n.2, p.49-64, 2011.
- GÜNTNER, A., & BRONSTERT, A. Large-scale hydrological modelling of a semiarid environment: model development, validation and application. In T. Gaiser, M. Krol, H. Frischkorn & J. C. Araújo (Eds.), *Global Change and Regional Impacts* (pp. 217-228). New York: Springer, 2003. http://dx.doi.org/10.1007/978-3-642-55659-3_17.
- HUANG, P.; LI, Z.; CHEN, J.; LI, Q.; YAO, C. Event-based hydrological modeling for detecting dominant hydrological process and suitable model strategy for semi-arid catchments. *Journal of Hydrology*, v. 542, p.292-303, 2016.
- KAN, G.; HE, X.; DING L.; LI, J.; LIANG, K.; HONG, Y. Study on Applicability of Conceptual Hydrological Models for Flood Forecasting in Humid, Semi-Humid Semi-Arid and Arid Basins in China. *Water*, v.09, n.10, 28 set. 2017. Disponível em:< <http://www.mdpi.com/2073-4441/9/10/719/pdf>>. Acesso em: 28 Dezembro 2017.
- KOKKONEN, T. S.; JAKEMAN, A. J.; YOUNG, P. C.; KOIVUSALO, H. J. Predicting daily flows in ungauged catchments: Model regionalization from catchment descriptors at the



Coweeta Hydrologic Laboratory, North Carolina, *Hydrological Processes*, 17(11), 2219–2238, 2003.

LI, H.; ZHANG, Y.; CHIEW, F. H. S.; XU, S. Predicting runoff in ungauged catchments by using Xinanjiang model with MODIS leaf area index, *J. Hydrol.*, 370(1–4), 155–162, 2009.

LIU, J.; HAN, D.: Indices for calibration data selection of the rainfall-runoff model, *Water Resources Research*, 46, W04512, 2010, DOI:10.1029/2009WR008668.

MCINTYRE, N.; AL-QURASHI, A. Performance of ten rainfall-runoff models applied to an arid catchment in Oman. *Environ. Model. Softw.*, 24 (6), 726–738, 2009.

MCINTYRE, N. R.; LEE, H.; WHEATER, H. S.; YOUNG, A. ; WAGENER, T. Ensemble predictions of runoff in ungauged catchments, *Water Resources Research*, 41, W12434, 2005, DOI:10.1029/2005WR004289.

MORIASI, D. N.; ARNOLD, J. G.; VAN LIEW, M. W.; BINGNER, R. L.; HARMEL, R. D.; VEITH, T. L. Model evaluation guidelines for systematic quantification of accuracy in watershed simulations. *American Society of Agricultural and Biological Engineers*, 2007. v. 50, n. 3, p. 885–900.

OLIVEIRA, G. A.; CIRILO, J. A.; BRITO, P. L.; NAIM, N. E. Qualidade do Posicionamento em Aplicativos VGI Obtido por Sensores de Localização em Smartphones. *Revista Brasileira de Cartografia*, V71, p806-831, 2019. Doi: 10.14393/rbcv71n3-49478.

UDIN, L.; ANDREASSIAN, V.; PERRIN, C.; MICHEL, C.; LE MOINE, N. Spatial proximity, physical similarity, regression and ungauged catchments: A comparison of regionalization approaches based on 913 French catchments, *Water Resources Research*, 44, W03413, 2008, DOI:10.1029/ 2007WR006240.

PARAJKA, J.; MERZ, R.; BLÖSCHL, G. A comparison of regionalisation methods for catchment model parameters, *Hydrology and Earth System Science*, 9(3), 157–171, 2005.

PARAJKA, J.; VIGLIONE, A.; ROgger, M.; SALINAS, J. L.; SIVAPALAN, M.; BLÖSCHL, G. Comparative assessment of predictions in ungauged basins – Part 1: Runoff-hydrograph studies. *Hydrology And Earth System Sciences*, v. 17, n. 5, p.1783-1795, 2013.

PATIL, S. D.; M. STIEGLITZ. Modeling daily streamflow at ungauged catchments: What information is necessary?, *Hydrological Processes*, 28(3), 1159–1169, 2014.

PERRIN, C.; MICHEL, C.; ANDRÉASSIAN, V. Improvement of a parsimonious model for streamflow simulation. *Journal of Hydrology*, v. 279, n. 1-4, p.275-289, 2003.

PILZ, T., DELGADO, J. M., VOS, S., VORMOOR, K., FRANCKE, T., COSTA, A. C., MARTINS, E., & BRONSTERT, A. (2019). Seasonal drought prediction for semiarid northeast Brazil: what is the added value of a process-based hydrological model? *Hydrology and Earth System Sciences*, 23(4), 1951-1971. <http://dx.doi.org/10.5194/hess-23-1951-2019>.

PINHEIRO, V. B.; NAGHETTINI, M. Calibração de um Modelo Chuva-Vazão em Bacias sem Monitoramento Fluviométrico a partir de Curvas de Permanência Sintéticas, *Revista Brasileira de Recursos Hídricos – RBRH*, v.15, n.2, p. 143-156, 2010.

PONCELET, C.; MERZ, R.; MERZ, B.; PARAJKA, J.; OUDIN, L.; ANDRÉSSIAN, V.; PERRIN, C. Process-based interpretation of conceptual hydrological model performance using a multinational catchment set. *Water Resources Research*, v. 53, n. 8, p.7247-7268, 2017.

PPRAFULLA, P.; YILMAZ, K.K.; GUPTA, H.V. Multiple-criteria calibration of a distributed watershed model using spatial regularization and response signatures. *Journal of Hydrology*, v. 418, p. 49–60, 2012. DOI:10.1016/j.jhydrol.2008.12.004

PUSHPALATHA, R.; PERRIN, C.; LE MOINE, N.; ANDRÉASSIAN, V. A review of efficiency criteria suitable for evaluating low-flow simulations. *Journal of Hydrology*, v. 420–421, p. 171–182, 2012. DOI:10.1016/j.jhydrol.2011.11.055.

REICHL, J. P. C.; WESTERN, A. W.; MCINTYRE, N. R.; CHIEW, F. H. S. Optimization of a similarity measure for estimating ungauged streamflow, *Water Resources Research*, 45, W10423, 2009, DOI:10.1029/2008WR007248.

RIBEIRO, A. A. S.; OLIVEIRA, G. A.; CIRILO, J. A.; BATISTA, L. F. D. R.; MELO, V. B. Floodplain reconstitution based on data collected via smartphones: a methodological approach to hydrological risk mapping. *Brazilian Journal of Water Resources*, v.25, p.1 - 13, 2020. Doi: 10.1590/2318-0331.252020190179.

RIBEIRO NETO, A.; CIRILO, J. A.; DANTAS, C.E.O.; SILVA, E. R. Caracterização da formação de cheias na bacia do rio Una em Pernambuco: simulação hidrológica-hidrodinâmica. *Revista Brasileira de Recursos Hídricos*, v.20, p.394 - 403, 2015.

SAMUEL, J.; COULIBALY, P.; METCALFE, R. A. Estimation of Continuous Streamflow in Ontario Ungauged Basins: Comparison of Regionalization Methods. *Journal of Hydrologic Engineering*, May 2011. DOI: 10.1061/(ASCE)HE.1943-5584.0000338

SEIBERT, J.; VIS, M. J. P. Teaching hydrological modeling with a user-friendly catchment-runoff-model software package, *Hydrology and Earth System Sciences*, 16(9), 3315–3325, 2012.

SELLAMI, H.; LA JEUNESSE, I.; BENABDALLAH, S.; BAGHDADI, N.; VANCLOOSTER, M. Uncertainty analysis in model parameters regionalization: A case study involving the SWAT model in Mediterranean catchments (Southern France), *Hydrol. Earth Syst. Sci.*, 18, 2393–2413, 2014. DOI:10.5194/hess-18-2393-2014.

SINGH, R.; ARCHFIELD, S. A.; WAGENER, T. Identifying dominant controls on hydrologic parameter transfer from gauged to ungauged catchments: A comparative hydrology approach, *J. Hydrol.*, 517, 985–996, 2014. DOI: 10.1016/j.jhydrol.2014.06.030.

TRAORE, V. B.; SAMBOU, S.; TAMBA, S.; FALL, S.; DIAW, A. T.; CISSE, M. T. Calibrating the Rainfall-Runoff Model GR4J and GR2M on the Koulountou River Basin, a Tributary of the Gambia River. *American Journal of Environmental Protection*, v. 3, n. 1, 20, p. 36-44, 2014.

VAN LIEW, M. W.; VEITH, T. L.; BOSCH, D. D.; ARNOLD, J. G. Suitability of SWAT for the Conservation effects assessment project: A comparison on USDA-ARS watersheds.



Journal of Hydrologic Engineering, v. 12, n. 2, p. 173-189, 2007.
[http://dx.doi.org/10.1061/\(ASCE\)1084-0699\(2007\)12:2\(173\)](http://dx.doi.org/10.1061/(ASCE)1084-0699(2007)12:2(173))

VIRAES, M. V.; CIRILO, J. A. Regionalization of Hydrological Model Parameters for the Semi-Arid Region of the Northeast Brazil. Brazilian Journal of Water Resources, v.24, p.e49, 2019. DOI: 10.1590/2318-0331.241920180114.

WANG, M.; ZHANG, L.; BADDOO T. D.; Hydrological Modeling in a Semi-Arid Region Using HEC-HMS. Journal of Water Resource and Hydraulic Engineering, v. 5, n. 3, p. 105-115, set. 2016.

WESTERBERG, I. K.; GUERRERO, J.-L.; YOUNGER, P. M.; BEVEN, K. J.; SEIBERT, J.; HALLDIN, S.; FREER, J. E.; XU, C.-Y.: Calibration of hydrological models using flow-duration curves, Hydrology and Earth System Science, 15, 2205-2227, 2011, <https://doi.org/10.5194/hess-15-2205-2011>

ZHANG, Y.; VAZE, J. ; CHIEW, F. H. S.; LI, M., Comparing flow duration curve and rainfall-runoff modelling for predicting daily runoff in ungauged catchments, Journal of Hydrology, 525, 72–86, 2015.